**J**ournal of **N**onlinear **A**nalysis and **O**ptimization
Vol. 13, Issue. 2 : 2022
ISSN : **1906-9685**


# EXAMINING THE INTERACTION BETWEEN SHOCK WAVES AND VISCOSITY IN TURBULENT MASS EJECTION EVENTS ON DECEMBER 18, 1999 AND APRIL 4, 2001

**[#1]Mr.AMMASI THIRUGNANAM,** *Assistant Professor*
**[#2]Mrs.BEERAM JAMUNA,** *Assistant Professor*
**Department of Physics,**
**SREE CHAITANYA INSTITUTE OF TECHNOLOGICAL SCIENCES, KARIMNAGAR, TS.**

## ABSTRACT
As a result of solar magnetic activity, shock waves and geomagnetic storms can be created by the discharge of magnetic field and plasma from the solar atmosphere, such as coronal mass ejections, or CMEs, and the solar wind. Shock waves are known to occur as solar particles shift from the supersonic to the subsonic zone. The interaction of shock waves and viscosity is largely relied on in space weather broadcasts, notably in the supersonic case of compressible gas flow. Thus, the primary purpose of this paper was to apply the modeling work from [1] to look for the viscosity consequence in the shocks discovered after the CMEs on December 18, 1999, and April 4, 2001.
***Keywords:*** Coronal mass ejection; viscosity; shock waves; reynolds number.

## INTRODUCTION
The photosphere, chromosphere, corona, and solar wind acceleration layers extend 100, 101, 101-102, and 103 mm from the solar surface, respectively. Corona, the solar atmosphere's outermost layer, is located above the chromosphere layer. Plumes, loops, and streamers raise the temperature of the corona from a few thousand to a few million Kelvins.
Coronas fascinate scientists because of their complex magnetically "closed" and "open" forms. According to Priest,the magnetic field and plasma interaction determine phenomena. Large plasma clouds known as CMEs can be expelled into interplanetary space when closed magnetic loops beneath coronal streamers grow. Coronal holes are caused by open plasma formations.
From the solar corona, a fast plasma stream from the fast solar wind travels to interplanetary space. Plasma will expand into the interplanetary medium at supersonic speeds as a solar wind at such high coronal temperatures predicted high-velocity solar wind approaching Earth in his seminal coronal expansion model. The first hypothesis was supported by theoretical advances and solar wind data. Recent plumes outside coronal holes have the potential to generate solar wind.Shock waves are produced when supersonic solar winds collide with the interplanetary medium. Solar wind shocks can be caused by CMEs, fast-slow stream interactions, and solar blast waves. They may, in fact, alter heat, compression, and magnetic field movements. After investigating the Kelvin-Helmholtz instability in the solar environment, Cavus and Kazkapan, found that the slow and rapid solar winds have radial speeds of 380 km/s and 780 km/s, respectively.
The Sun's continual particle outflow, the solar wind, collides with the planet's atmosphere to form a shock wave on the sunward side. Shock waves from solar wind particles can travel at speeds of 350-700 km/s, which is substantially faster than the interstellar medium's speed of 100 km/s.and Stepanova and Kosovichev used the Solar and Heliospheric Observatory/The Large Angle and Spectrometric Coronagraph (SOHO/LASCO) project to detect CMEs and solar wind

shocks. Because expanding ejects travel faster than the ambient gas before or behind them, there will be a shock ahead and a decreasing speed distribution inside the ejects. Kilpua et al. found a link between shock characteristics and density compression.

The undisturbed solar wind affects the forward frontal structure of the CME, as demonstrated by Eselevich & Eselevich. As the CME moves away from the Sun, a narrow discontinuity region appears near the front's disturbed zone. Collisions occur at radial distances less than 6RSun and are collisionless at distances greater than 6RSun (where r is the distance from the Sun's center and RSun is the solar radius).

Some case studies on shock waves addressed the complex entropy behavior. Investigated the entropy profile through shock without viscosity and heat conduction effects. They discovered that entropy increases in the shock front to its maximum at the center and then drops in the other half. This appears to be a violation of the second law of thermodynamics, but it applies to the entire system because entropy increases downstream of the shock wave. Then investigated shock wave entropy in a standard dusty gas Navier-Stokes equation model. He discovered that the shock front has the largest entropy distribution, which increases with upstream Mach number and particle density. Using the model I for example, investigated entropy in the shock wave after the 12/12/2006 CME.

NASA's Advanced Composition Explorer (ACE) spacecraft observes these occurrences on a regular basis. The Sun-Earth L1 libration point (240 times Earth radius) will be orbited by the ACE observatory, a 5-rpm rotating spacecraft. The ACE spacecraft has gone approximately 1.5 million kilometers to escape Earth's magnetic field. investigated shock waves following CMEs on 18 February 1999 and 28 April 2001, which were accompanied by flares and coronal waves. This research applies the models to the shock wave generated by these CMEs. Physical parameter measurements from the ACE mission are used as upstream conditions.

The model was developed to study and predict Earth shock waves. This study looks into the effect of viscous flows on the shock wave after these two CMEs. To characterize shock processes, the hydrodynamic model in solves the Navier-Stokes equations. This modeling technique takes into account the viscous behavior of gas as a function of Reynolds number discusses the downstream shock waves from the CMEs that occurred on February 18, 1999 (CME18/02/1999) and April 28, 2001 (CME28/04/2001).Gary and Matthaeus et al. [28] characterize the wind acceleration zone as infinite, ranging from 44 to infinity. Gonzales-Esparza et al. reconsider the importance of gas pressure in the dynamical modeling of solar wind.

The CME interval is indicated by the recombination of enhanced density, temperature, and velocity profiles. Table 1 provides upstream parametric values from the ACE satellite for shocks following CME18/02/1990 and CME28/04/2001. They are used in model to investigate shock viscosity effects.

Density measurements frequently anticipate the occurrence and arrival of a shock. CME18/02/1999 and CME28/04/2001 had estimated velocities of 390 and 445 km/s, respectively, in Table 1. Because the interplanetary medium's local sound speed is around 100 km/s the shock wave should begin in this region between 1x105 and 5x104 Kelvin (Table 1).

## MODEL FORMULATION

### Physical Parameters

The plasma parameter—the ratio of plasma pressure to magnetic pressure—describes complex plasma and magnetic pressures in the solar environment. Plasma pressure trumps magnetic pressure if is greater than one. This ratio is modified by the magnetic field, which is >>1 in the solar wind acceleration zone while Matthaeus et al. found 44 to infinity. Gonzales-Esparza et al. reconsider gas pressure in solar wind dynamical modeling.

The CME interval is characterized by heightened density, temperature, and velocity profiles recombining. Table 1 and show ACE satellite upstream parametric values for shocks after

CME18/02/1990 and CME28/04/2001 model investigates shock viscosity effects with them.
Density measurements often predict shocks Table 1 shows estimated velocities of 390 and 445 km/s for CME18/02/1999 and CME28/04/2001. The interplanetary medium's local sound speed is 100 km/s hence the shock wave should start between 1x105 and 5x104 Kelvin (Table 1).

**Basic Formulae**

The plasma $\beta$ parameter defined as,

$$\beta = \frac{p_{gas}}{p_{mag}} \qquad (1)$$

have values greater than one in the solar since magnetic pressure is dominated by plasma gas pressure at high coronal temperatures. The wind problem is thus reduced to the hydrodynamic scenario discussed.

As a result, for a larger viscous shock in constant flow [1,]

$$[(\frac{1}{2}-\frac{4}{3}\frac{1}{Re_1})(\gamma-1)M_1^2+1]\kappa^2-[(1-\frac{4}{3}\frac{1}{Re_1})\gamma M_1^2 \qquad (2)$$
$$+1]\kappa+(\frac{\gamma+1}{2}-\frac{4}{3}\frac{1}{Re_2})M_1^2=0$$

Table 1. Upstream values of physical parameters for two different shocks, after the CME18/02/1990 and CME28/04/2001

| | $n_1$(cm$^{-3}$) | $T_1$(Kelvins) | $u_1$(km/s) |
|---|---|---|---|
| CME18/02/1999 | 3 | 1x10$^5$ | 390 |
| CME28/04/2001 | 3.43 | 5x10$^4$ | 445 |

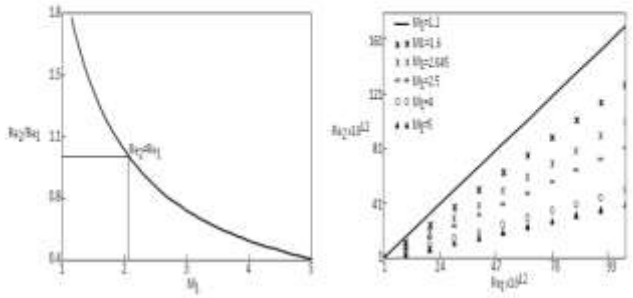

Fig. 1. Changes of the downstream Reynolds number ($Re_2$) as a function of the upstream Mach number $M_1$ (left) and the upstream Reynold's number $Re_1$ (right)

Upstream and downstream Reynolds values (Re1 and Re2, denoted by subscripts 1 and 2) are used in Equation (2). There is a specific heat ratio (), a downstream-upstream density ratio (K), and an upstream Mach number (M1). The parametric values M1, Re1, and Re2 influence the distributions of downstream physical parameters. Eselevich and Eselevich discovered that for collisionless shocks is 5/3 3. The downstream physical parameter values were obtained using Rankine-Hugoniot jump formulas. It is stated how fluid states on both sides of a shock wave interact. Pressure ratios to compression rate, like Cavus and Kurt can be used to quantify entropy (S2-S1) changes:

$$S_2 - S_1 = c_v \ln[\frac{p_2}{p_1}\kappa^{-\gamma}] \qquad (3)$$

**Downstream Reynolds Numbers in the Solar Wind**

As a result, the Reynolds number (Re>>1) of the solar wind influences the behavior of this region. In the solar wind speeding up region represent a jump to 1012 and 1014.

As a function of, Re1, and M1, the downstream Reynolds number, Re2, is simplified. The ratio Re2/Re1 falls as the upstream Mach number increases until it hits unity (Re1=Re2) for M12. This zone transitions from mild to severe shocks, with M12 for mild shocks and M1>2 for severe shocks.

The right panel of Fig. 1 shows the variation of Re2 based on Re1 for various M1 values for a

monatomic gas with =5/3. According to Borovsky and Funsten and Veselovsky the Reynolds number Re2 increases with Re1 and decreases with M1.

**MODELLING RESULTS FOR THE SHOCKS HAPPENED AFTER THE CME18/02/1999 AND CME28/04/2001**

The symbolic and numeric computing environments Maple 9.5 were used to adapt various solutions of the equations (2-3) and Rankine-Hugoniot jump formulas [34] to determine the downstream parameter values for shock waves induced by the CME18/02/1999 and CME28/04/2001. Table 2 or Figures 2-8 indicate the downstream physical parameters. For solar wind simulations, we use the upstream Reynolds number of 1013.

Table 2. Variations of the basic physical parameters as a function of $M_1$

| $M_1$ | $Re_2/Re_1$ | $n_2/n_1$ | $u_2/u_1$ | $T_2/T_1$ | $S_2$-$S_1$ | $M_2/M_1$ |
|---|---|---|---|---|---|---|
| 1.200 | 1.704 | 1.297 | 0.771 | 1.195 | 0.055 | 0.705 |
| 1.600 | 1.278 | 1.842 | 0.543 | 1.602 | 0.798 | 0.429 |
| 2.045 | 1.000 | 3.329 | 0.437 | 2.137 | 2.441 | 0.294 |
| 2.500 | 0.818 | 2.703 | 0.370 | 2.798 | 4.566 | 0.221 |
| 4.000 | 0.511 | 3.368 | 0.297 | 5.863 | 11.961 | 0.123 |
| 5.000 | 0.409 | 3.571 | 0.280 | 8.680 | 16.368 | 0.095 |

The basic physical model is parameterized in Table 2 as a function of M1. Reynolds number ratios (Re2/Re1), density ratios (n/n), and velocity ratio (u/u) are proportional to increasing Reynolds number ratios. This variation appears linear for mild shocks (M12) but nonlinear for large shocks (M1>2). As established by equation (1) and jump situations, n2 reaches 10 cm-3 for temperature (T2/T1), Mach numbers ratio (M2/M1), and entropy differential (S2-S1). When the Reynolds number ratio is equal to one, the critical Mach number for the turning point is M1=2.045 (Fig. 1). According to Cavus this location influences shock wave strength and the Reynolds number ratio. After reaching M1=2.045, the decreasing trends of Re2/Re1, u2/u1, and M2/M1 begin to level out. Density, temperature, and entropy discrepancies, on the other hand, increase with M1, slowing for n2/n1 and speeding up for T2/T1 and S2-S1 after M1=2.045.

The downstream density dependence as a function of M1 and Re2/Re1 are derived from the upstream density values in Table 1 and shown in the left and right panels of Fig. 2. As the upstream Mach number increases, so does n2, whereas density falls (CME18/02/1999, 12 cm-3 for CME28/04/2001). (Fig. 2).

Figure 3 depicts downstream temperature variations as a function of M1 and Re2/Re1. The weak shock zone (M12) changes less than the strong shock region (M1>2). Table 1 offers upstream temperature values (1105 and 5104 Kelvin) for determining downstream temperature T2, which increases with upstream Mach number M1=5, fluctuates slightly for M12, and increases again for M1>2 (refer to Table 2). T2 values of 8.68106 Kelvin and 4.34105 Kelvin arise from higher M1 values (CME18/02/1999 and CME28/04/2001, respectively).

Figure 4 depicts downstream velocity u2 as a function of M1 (left panel) and Re2/Re1. Table 1's upstream values both decrease. Unlike T2, u2 drops dramatically for small shocks (M12) compared to large shocks (M1>2).

Fig. 2. Changes in the downstream density (in $cm^{-3}$) as a function of $M_1$ (left) and $Re_2/Re_1$ (right) for both the CME18/02/1999 and CME28/04/2001

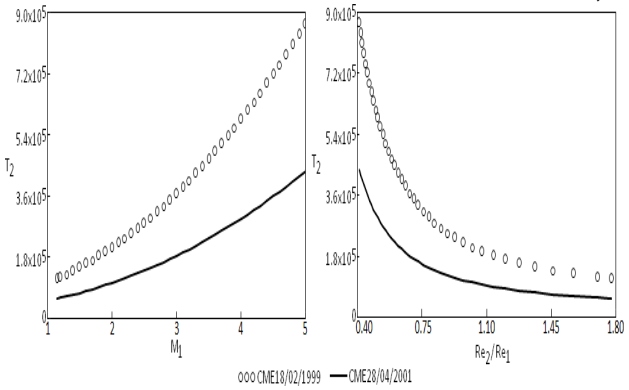


Fig. 3. Downstream temperature changes $T_2$ (in Kelvin) drawn as a function of $M_1$ (left) and $Re_2/Re_1$ (right) values of CME18/02/1999 and CME28/04/2001

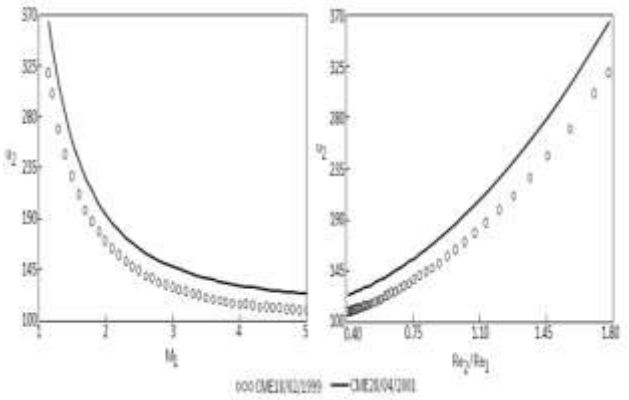

Fig. 4. Variation of $u_2$ with respect to $M_1$ (left) and $Re_2/Re_1$ (right) values

In fig. 5, the cross symbols representing temperature ratios of downstream to upstream values (T2/T1) increase with entropy difference. The empty squares represent the compression ratio (n2/n1), which rises with sound speed, whereas the empty triangles represent the Re2/Re1 ratio, which falls. Furthermore, when entropy differences grow larger, plus signs suggest decreasing downstream-to-upstream velocity ratios (u2/u1). For isentropic S2-S1=0, all ratios are equal to one. In the isentropic scenario (S2-S1=0), all ratios become one, suggesting that there is no shock in the absence of compression (=1).

Figure 6 depicts downstream density shift based on entropy difference, with S2-S12.44 corresponding to Table 2's weak shock (M12) region. Downstream density variations (n2) increase with entropy differences S2-S1, as expected, but they are small for future S2-S1 increases. T2's S2-S1 dependency, on the other hand, increases with entropy differences in Fig. 7. T2 changes are lower in the mild shock zone (S2-S12.44) than in the strong shock zone (S2-S1>2.44).

In Fig. 8, downstream velocity (u2) drops as expected with entropy differences (S2-S1), yet u2 variations are minor for substantial differences. When M1>>2, strong shocks show significant variance, while extremely weak shocks are almost isentropic when S2 is approximately equal to its upstream value in Table 2.

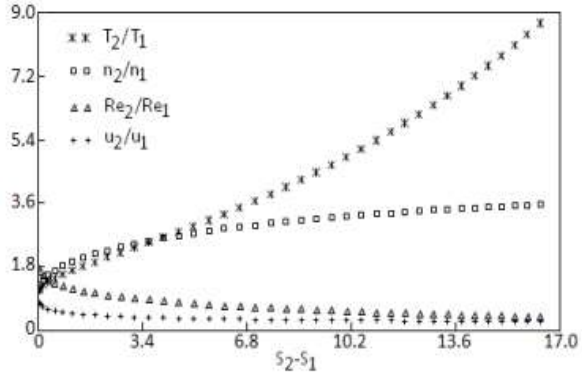


Fig. 5. Variations of some parameters with respect to the entropy difference $S_2$-$S_1$

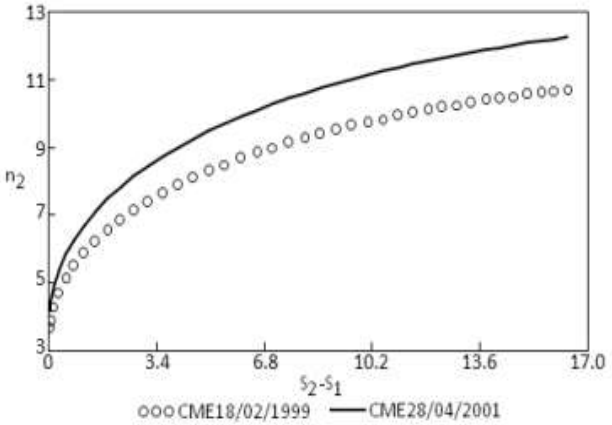


Fig. 6. Downstream density variation with respect to entropy difference $S_2$-$S_1$ for CME18/02/1999 and CME28/04/2001

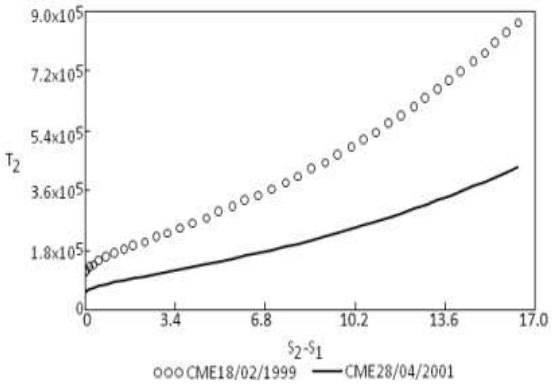


Fig. 7. Variations o $T_2$ as a function of $S_2$-$S_1$ for the CME18/02/1999 and CME28/04/2001

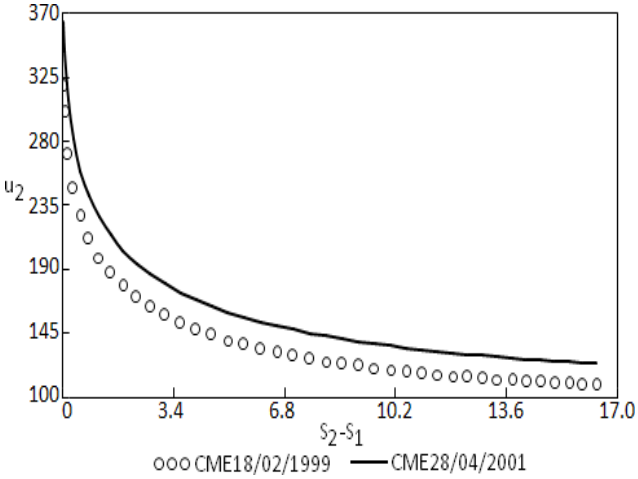


Fig. 8. Variations of $u_2$ as a function of $S_2$-$S_1$ for the CME18/02/1999 and CME28/04/2001

## DISCUSSION AND CONCLUSION

Because enough energy is released quickly to form a "fast" CME, understanding CME-driven shock waves from the Sun to interplanetary space is required for space weather predictions. Based on current observational data, characterizing behavior and physical characteristics is difficult.

Corona CMEs are known to cause complex magnetic, thermal, and interplanetary plasma interactions. Regardless of magnetic pressure, gas pressure reigns supreme beyond the Sun. The solar wind CME-driven shock can be studied using hydrodynamic simulation.

This study looks at shock waves that occurred following CMEs on February 18, 1999 and April 28, 2001. A 1-D hydrodynamical model with Reynolds number effects is used to investigate shock propagation in space. Conclusions based on our findings:

When compared our downstream plasma density of 10.3 cm-3 fits Figure 2's M14.4. M14.9 is predicted by our model, with a downstream density of 12.2 cm-3. These shock parameters are consistent with the severe shocks (M1>4) predicted for CME18/02/1999 and CME28/04/2001. The magnitude of these shocks demonstrates that our theoretical models correspond to ACE satellite data.

The shocks have Reynolds number ratios (Re2/Re1) of 0.46 and 0.41, respectively, as illustrated in Fig. 1. For both CMEs, the upstream is more turbulent than the downstream (Re2Re1).

The kinematic viscosity ratio (1/2) is increased by Re2/Re1. The velocities increase upstream of the shock (1>2). Figures 2 and 3 show decreasing T2 and n2 with rising 1. In Figure 4, downstream velocity (u2) increases with 1/2 as expected.

Both shock waves compressed at a rate of 3.5. Aftershock velocities for CME18/02/1999 and CME28/04/2001 should be 112 and 125 km/s, respectively (Fig. 5).

Using upstream Mach values of 4.4 and 4.9 and upstream velocities in Table 1, the two scenarios' sound speeds in the interplanetary medium are 89 km/s and 91 km/s, respectively, which are similar to which anticipated 90-100 km/s.

The entropy differential S2-S1 grows as the upstream Mach number M1 increases. Weak shocks (M12.2), like, become isentropic as Reynolds number ratios (Re2/Re1) grow.

S2-S1 entropy difference increases with compression rate (), indicating that entropy difference enhances downstream density. Disparities in entropy raise downstream temperature. Unlike temperature ratio changes, entropy disparities S-S decreases as fluid velocity ratios increase.

## REFERENCES

1. Cavus H. On the effects of viscosity on the shock waves for a hydrodynamical case — Part I: Basic Mechanism Advances in Astronomy. 2013;2013. DOI: 10.1155/2013/58296).
2. Parker EN. Heating solar coronal holes The Astrophysical Journal. 1991;372:719- 727. ejections. Advances in Space Research. 2006;38:535-546.
3. Kilpua EKJ, Isavnin A, Vourlidas A, Koskinen HEJ, Rodriguez L. On the relationship between interplanetary coronal mass ejections and magnetic clouds, Annales Geophysicae. 2013;31:1251- 1265.
4. Eselevich V, Eselevich M. Disturbed zone and piston shock ahead of coronal mass ejection. The Astrophysical Journal. 2012; 761(68):1-10.
5. Morduchow M, Libby PA. On a complete solution of the one-dimensional shock wave structure. J. Aeron. Sci. 1949;16: 674-684.
6. Hamad H. Behavior of entropy across shock waves in dusty gases, Zeitschrift für angewandte Mathematik und Physik. 1998;49:827-837.
7. Cavus H, Kurt A. Effects of viscosity on the behavior of entropy change in the shock wave that occurred after the December 13, 2006 coronal mass ejection. Astrophysical Bulletin. 2015;70:220-225.